1. Title page

The respective impacts of chemo- and radiotherapy on microglia in the brain

A thesis submitted in partial fulfilment of the

HONOURS DEGREE of BACHELOR OF

HEALTH AND MEDICAL SCIENCES In

The Discipline of Physiology

Adelaide Medical School

The University of Adelaide

By Vivien Heng

November 2020

3. Abstract

Background: Cancer therapies have been shown to lead to cognitive impairments and is believed to involve early M1 proinflammatory microglial activation, a well-established indicator of neuroinflammation. IBA1 is a specific and established microglia marker, but the emerging marker for activated microglia, TSPO, can be used in live-imaging. We investigated the feasibility of using TSPO to determine activated microglia following chemo- and radiotherapy.

Methods: Female and male C57Bl/6 mice were treated with 5-fluorouracil (5-FU) 400 mg/kg vs saline (n=24), and culled between Day 1 and 32; or with 2 Gy and sham radiation and culled at Day 2 (n=7). Immunofluorescence staining was performed on brain sections for IBA1 and TSPO expression. The cerebellum, hippocampus dentate gyrus, CA1 and CA3, and prefrontal cortex were analysed by IBA1+ and TSPO+ cell counts and morphology index ratios in ImageJ.

Results: TSPO+ counts increased significantly in the cerebellum and hippocampus 5FU Day 1 to 32 from 9.0±5.3 to 47.0±11.4, P=0.012; 14.3±4.5 to 76.7±25.5, P=0.0007 respectively. Counts also significantly increased in the cerebellum, hippocampus and prefrontal cortex, in controls Day 1 to 32 from 11.0±9.5 to 47.7±6.7, P=0.016; 14.3±3.5 to 88.3±22.5, P=0.0001; 39.3±16.3 to 97.7±38.55, P=0.033, respectively. No significant differences were observed in IBA1+ cell counts beyond prefrontal cortex controls, between radiotherapy counts in treated and control animals, or in chemotherapy IBA1+ morphology index ratios.

Conclusion: Our study found that TSPO+ but not IBA1+ cells increase with time in brain regions associated with cognitive impairment following chemotherapy, while both did not increase following radiotherapy.

3. Introduction

3.1 Background

Cancer-related cognitive impairments (CRCI), such as problems with memory and focus, chronically affect up to 75% of non-central nervous system cancer survivors, lasting up to 20 years

after treatment for 1 in 4 survivors[1]. The cancer therapies chemo- and radiotherapy have been shown to lead to cognitive impairments and structural brain changes in humans[1, 2]. Based on various animal studies, the mechanisms responsible are believed to involve early proinflammatory microglial activation, a well-established indicator of neuroinflammation[3, 4]. 'Activated' microglia may refer to either the M1 proinflammatory or M2 anti-inflammatory phenotypes; unless otherwise specified, for the purposes of this thesis 'activated' microglia will refer to the M1 phenotype[5].

A moderate number of rodent studies have investigated microglial changes in the brain induced by chemo- and/or radiotherapy[3, 4, 6-12]. Methotrexate was predominantly used as the chemotherapy, while radiotherapy was mostly head-targeted. These studies reported impacts on microglial number and/or morphology. The predominant analytical method was immunohistochemistry staining for ionised calcium binding adaptor molecule 1 (IBA1), a specific and established marker of resting and activated microglia[13]. The less commonly used methods include the immunohistochemical staining of another activated microglia marker, CD68[4, 6, 9, 10, 12], microfluidic qPCR for activated microglial gene transcripts[6], and [11C]PK11195 radiotracer detection[11]. Most studies have reported evidence for neuroinflammation, with a general increase in microglial numbers and morphological changes involving larger microglial bodies and thicker processes. Some studies reported decreases in microglial numbers in various areas shortly after chemotherapies cyclophosphamide, docetaxel, 5-fluorouracil (5-FU), or topotecan in the prefrontal cortex[8], or after whole-brain radiation in the dentate gyrus[9] compared to controls. The microglia impacts varied between brain regions, chemo- and radiotherapy doses, time of cull and age of animals.

Limited understanding of the role of microglia in the pathogenesis of CRCI is due to a lack of consistency between studies in terms of type and dose of treatments, timing of investigation, tissue preparation and analyses, and brain regions assessed. Further, most studies only address chemo- or radiotherapy when both are used in cancer treatment, and there is a lack of non-brain directed radiation therapy (NBRT) models[3]. Dey et al. 2020 found that the combination of

temozolomide chemotherapy and whole-brain radiation leads to an acute increase in activated microglia in the hippocampus[4]. Feiock et al. 2016 reported that the neuroinflammatory response defined by microglial numbers and morphological changes induced by methotrexate versus NBRT, were statistically indistinguishable. There were increased numbers of IBA1-positive microglia in the rostral cortex, striatum, cerebellum, hippocampus and medulla, with morphological changes aligned with activation[3].

Compared to methotrexate, limited studies have investigated the microglial changes induced by chemotherapeutic 5-FU, which has been shown to induce cognitive impairments in patients and animal models[14]. It has been seen to reduce neurogenesis in the hippocampus in rodents[15], and it, as well as its derivatives have contributed to white matter changes reported in patients[16]. 5FU is frequently used to treat breast, cervix and gastrointestinal cancers[14, 17] and is small enough to potentially cross the blood brain barrier, which may facilitate its damage to the brain[14].

The limitation with existing methods in pre-clinical CRCI research, which rely on immunohistochemical detection of markers, is the requirement of necropsy tissue, which only allows one time point per animal and post-mortem assessment. There is an emerging marker for neuroinflammation, the upregulation of mitochondria outer membrane translocator protein (TSPO), which has been suggested to be involved in immune function and energy production[18]. However, there has been a debate as to whether the upregulation of TSPO signifies pro- or anti-inflammatory phenotypes in glial cells[19]. TSPO has been used in live-imaging and *in vitro* studies, as well as in clinical diagnosis[18-20], and current evidence is highly promising towards the upregulation of TSPO in proinflammatory glial cells[19].

TSPO is largely undetectable in resting microglia by the current available techniques, however is greatly upregulated with neuroinflammation and microglial activation[20, 21]. Neuroinflammation can be detected using PET imaging with TSPO radiotracers *in vivo* and *in vitro*[22]; the *in vivo* live-imaging aspect is particularly beneficial as the progress of neuroinflammation (e.g. microglial activation) can be taken without sacrificing animals, which is

more clinically applicable than existing methods. However, the disadvantages of using TSPO to identify activated microglia is that it is expressed in other cells, including astrocytes, endothelial cells and pericytes, [19, 23, 24]. Thus, while TSPO does have its advantages over IBA1 immunohistochemical staining, it is not specific to microglia, which complicates the interpretation of expression and imaging results. Before TSPO can progress into clinical diagnostic protocols, a deeper understanding of the cells it detects, as well as its relationship to neuroinflammation following chemo- and radiotherapy is required.

Ultimately, what remains unknown are the similarities and differences between the neuroinflammatory response induced between chemo- and NBRT radiotherapy, both of which are comparable as they are non-brain directed and systemic[25]. And further, whether TSPO expression reflects the respective neuroinflammatory responses.

3. 2 Hypothesis and aims

I hypothesised that chemo- and radiotherapy respectively, will have comparable neuroinflammatory responses, which will be detectable via TSPO expression. To address my hypothesis, I aimed to determine IBA1 and TSPO expression in the brain following chemo- and radiotherapy exposure, respectively.

4. Materials & Methods

4.1 Ethics approval

The chemotherapy study was approved by the South Australian Health and Medical Research Institute (SAHMRI) Animal Ethics Committee SAM435.19. The radiotherapy study was approved by the University of Sydney Animal Ethics Committee and the Australian Nuclear Science and Technology Organisation (ANSTO) Animal Care and Ethics Committee, Animal Research Authority P301. All procedures were aligned with the Australian Code of Practice for the Care and Use of Animals for Scientific Purposes (8th edition, 2013).

4.2 Animal models

All mice were housed with free access to food and water, under 12-hour light/dark cycle.

In the chemotherapy study, 13-15-week old C57Bl/6 female mice obtained from SAHMRI Bioresources (South Australia) were treated with 5-FU 400 mg/kg[17] vs saline (control) via intraperitoneal injection (n=24) and followed up to 32 days. Mice were anaesthetised with 5% (v/v) of isoflurane and humanely culled by pentobarbitone overdose 125 mg/kg and transcardial saline perfusion. The treated mice were culled at Day 1, 2, 4, 8, 16, and 32, while the control mice were culled at Day 1 and 32 (n=3 per day per treatment); Day 1 represents 24 hours, and so on. A broad range of cull points were selected to address the inconsistency of investigation points in the literature.

In the radiotherapy study, 6-week-old C57Bl/6 healthy male mice obtained from the Animal Resource Centre (Western Australia) were treated with 2 Gy[4] of whole-body gamma radiation at a dose of 0.08 Gy/minute (n=3) vs sham radiation (control) (n=4). Mice were humanely culled via isofluorane overdose and exsanguination on Day 2 after irradiation, at which microglial activation was previously demonstrated to peak in unpublished preliminary data from our collaborator's laboratory.

4.3 Tissue preparation

In the chemotherapy study, brains were collected and fixed in 4% buffered paraformaldehyde and embedded in paraffin. 5 μm sagittal sections at the level of the cerebellum, hippocampus, and prefrontal cortex, were obtained on a rotary microtome (Leica RM2235). Sections were floated in water at 38°C, placed on coated Flex IHC microscope slides (DAKO, Carpinteria, CA, USA). The tissue mounted slides were heated in an oven at 38°C overnight, then dewaxed in 3 rounds of histolene for 5 minutes each, and rehydrated through graded ethanol 100, 90, and 70% for 1 minute each.

In the radiotherapy study, brains were snap frozen in liquid nitrogen and stored at -80°C. 10 μm coronal sections at the level of the hippocampus were obtained on a cryostat (Leica CM3050) at

-18 to -20°C. Sections were placed on Poly-lysine slides (Thermo Scientific, Rockford, IL, USA) and stored at -80°C until use[24]. The tissue mounted slides were blow dried for at least 30 minutes with cool air before staining. Tissue sections were fixed with 3.7% formaldehyde in PBS for 5 minutes, then permeabilised with ice-cold acetone[24].

4.4 Immunofluorescence

Antigen retrieval was required for the chemotherapy study tissue, but not the radiotherapy, and was performed for 20 minutes at 97°C with a Tris-EDTA buffer (pH 9.0) in a DAKO PT Link water bath.

Immunofluorescence staining for all tissue sections was performed on the DAKO Austostainer Plus, serial number AS1271F1104 (Via Real, California, USA). Tissue sections were twice rinsed with 1xPBS buffer. Non-specific antibody binding was blocked with 5% goat serum and 5% bovine serum albumin (BSA) in 1xPBS[24] for 60 minutes, followed by an air blow then buffer rinse. Primary antibodies rabbit TSPO rabbit monoclonal antibody (ab109497, Abcam)[24] and rabbit anti-Iba1 antibody (#019-19741, Wako)[26], were applied for 60 minutes at the concentration 1:200 (from stock 1 μg/mL and 0.5 μg/mL respectively) to separate sets of corresponding tissue, followed by two 1xPBS buffer rinses. Secondary reagent Alexa Fluor 488 goat anti-rabbit IgG (ThermoFisher, Invitrogen, Catalog # A-11034) was applied at concentration 1:1000 (from 2 mg/mL stock) for 60 minutes, followed by two 1xPBS buffer rinses. The nuclear stain 4′,6-Diamidino-2-phenylindole dihydrochloride (DAPI) (Sigma-Aldrich, Saint Louis, MO, USA, Catalog # D9542 and D8417) was applied at concentration 1:1000 (from 2 mg/mL stock) for 15 minutes, followed by two 1xPBS buffer rinses. Sections were then mounted in Fluoroshield F6182 (Sigma-Aldrich, Saint Louis, MO, USA) and coverslipped with 22x22mm #1.5 coverslips Thermo Scientific Menzel Gläser 630-2884 (Germany).

4.5 Haematoxylin and eosin (H&E)

H&E staining[10, 27] was performed on the tissue sections subsequent to tissue preparation on Superfrost microscope slides (Menzel-Gläser, Germany) for the chemotherapy study, and Poly-lysine slides (Thermo Scientific, Rockford, IL, USA) for the radiotherapy study.

4.6 Microscopy

Scans for whole tissue sections were obtained at 40x objective via the Zeiss Axio Scan.Z1 slide scanner (Germany) for the immunofluorescent stained tissue, and the Nanozoomer (Hamamatsu Photonics, Japan) for the H&E stained tissue.

4.7 Quantification

Immunofluorescence images of 0.06mm^2 for analysis were obtained via ZenBlue 3.1. Positively stained cells and fragments for IBA1 and TSPO were counted[7] by one observer and tallied via the Cell Counter plugin on ImageJ-win64, including cell bodies and fragments that were brighter than the background in the images. Morphological index of IBA1-postive cells were manually determined for microglia-like cells with clear soma and nuclei in the chemotherapy tissue. Any cells that were only partially captured due to the boundaries of the images were discounted. Morphological index was obtained via the average ratio of the soma area and the arborisation area (area created by joining the tips of the processes of a microglia cell) via ImageJ-win64[28]. The radiotherapy tissue was excluded from morphological index analyses as fluorescence images obtained via the Zeiss Axio Scan.Z1 slide scanner did not show obvious microglia-like structures; however, presence of microglia-like cells was confirmed via the Olympus FLUOVIEW FV3000 confocal microscope at 60x objective (data not shown).

4.8 Statistical analyses

Data was statistically analysed for significance via GraphPad Prism 8. Data passed the Shapiro-Wilk test for normality. One-Way ANOVA with *post hoc* testing via Tukey's multiple comparisons was performed on the chemotherapy counts, Day 1 to 32 treated and controls for cerebellum, hippocampus CA1 and prefrontal cortex. Unpaired, parametric, two-tailed t-test was

performed on radiotherapy counts Day 2 treated and control, corresponding chemotherapy counts Day 1 control and Day 2 treated, and IBA1 chemotherapy morphology data for hippocampus regions dentate gyrus, CA1 and CA3. Significance was considered at level of *P≤0.05, **P≤0.01, ***P≤0.001, ****P≤0.00001, and data was represented as mean±SD

6. Results

6.1 IBA1+ and TSPO+ staining

IBA1+ and TSPO+ immunofluorescence staining was identified via channel green staining for the chemo- cerebellum (Figure 1), hippocampus CA1 (Figure 2) and prefrontal cortex (figure not shown); and radiotherapy (Figure 3, 4, 5) tissues, which represented the fluorophore Alexa Fluor 488 and indicated the binding of IBA1 and TSPO antibodies, respectively.

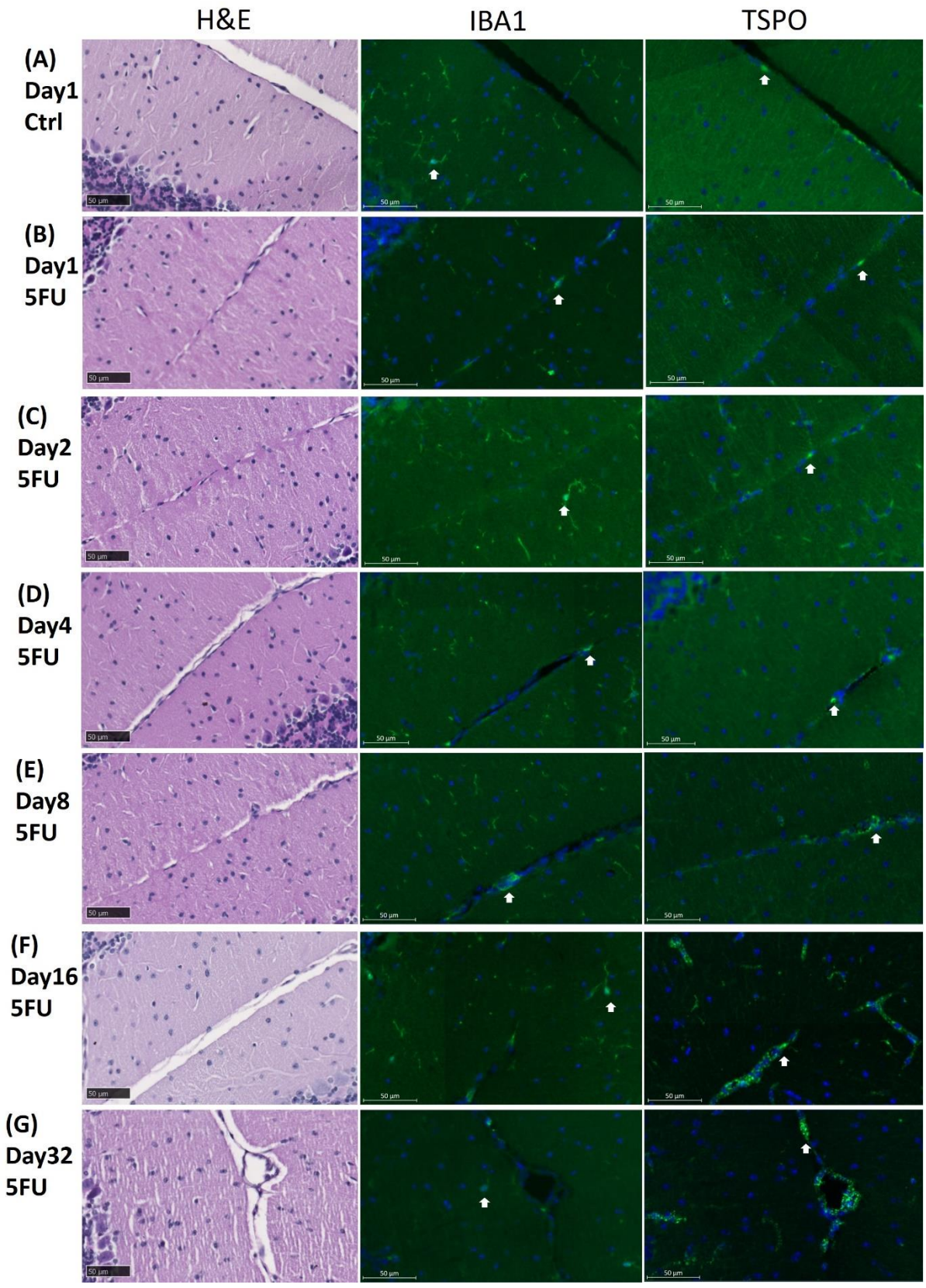

Figure 1. Left to right: H&E, IBA1 and TSPO immunofluorescence staining of chemotherapy cerebellum at 40x objective. Top to bottom, rows represent (A) Day1 Ctrl, (B) Day1 5FU, (C) Day2 5FU, (D) Day4 5FU, (E) Day8 5FU, (F) Day16 5FU, and (G) Day32 5FU. Day32 Ctrl not

included. Arrows examples of binding of IBA1 or TSPO antibodies. The blue in IBA1 and TSPO represents DAPI staining; the green represents the fluorophore Alexa Fluor 488, and indicates the binding of IBA1 and TSPO antibodies respectively.

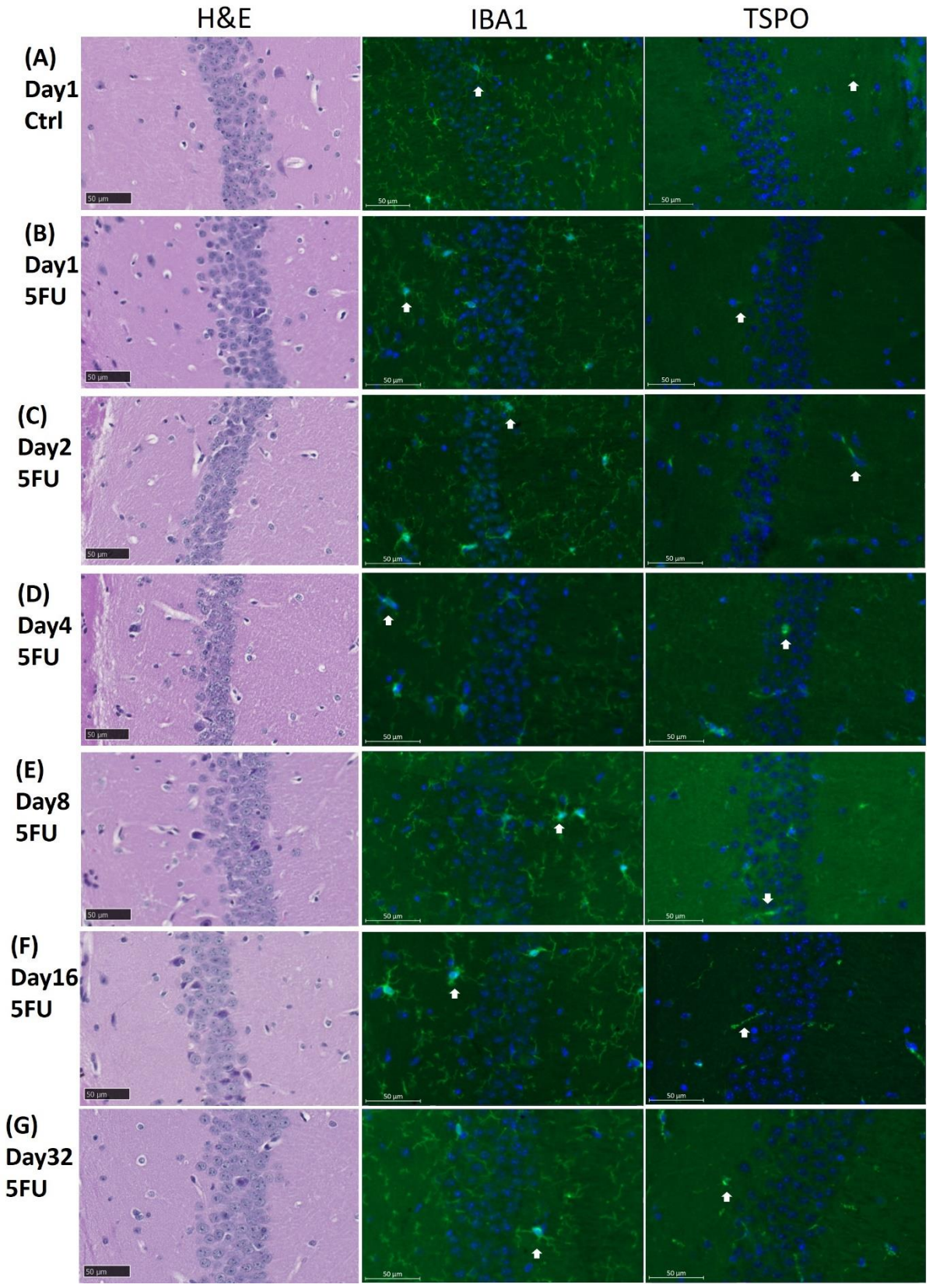

Figure 2. Left to right: H&E, IBA1 and TSPO immunofluorescence staining of chemotherapy hippocampus CA1 at 40x objective. Top to bottom, rows represent (A) Day1 Ctrl, (B) Day1 5FU, (C) Day2 5FU, (D) Day4 5FU, (E) Day8 5FU, (F) Day16 5FU, and (G) Day32 5FU. Day32 Ctrl not included. Arrows examples of binding of IBA1 or TSPO antibodies. The blue in IBA1 and TSPO represents DAPI staining; the green represents the fluorophore Alexa Fluor 488, and indicates the binding of IBA1 and TSPO antibodies respectively.

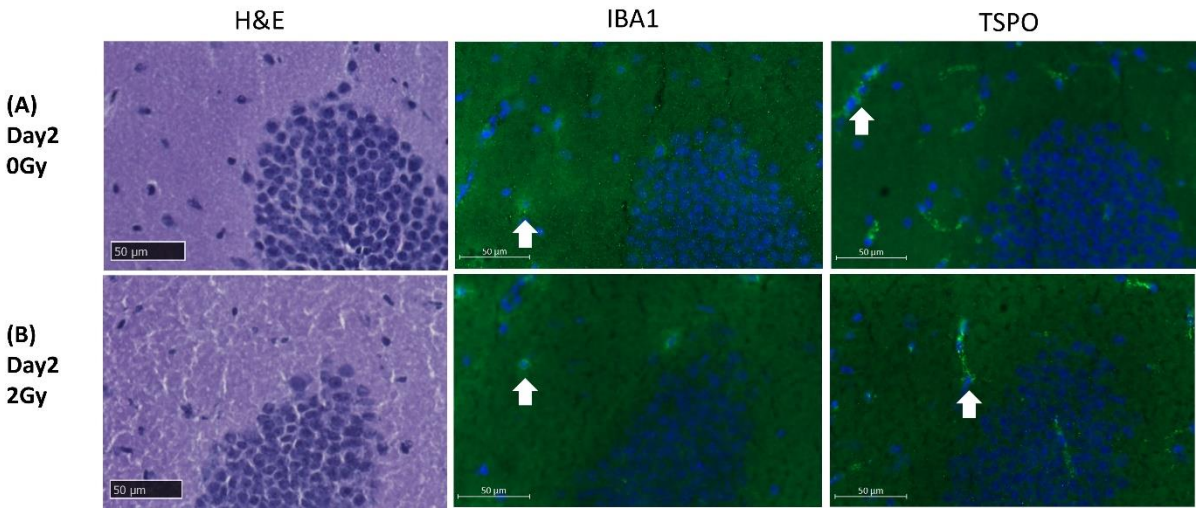

Figure 3. Left to right: H&E, IBA1 and TSPO immunofluorescence staining of radiotherapy dentate gyrus at 40x objective. From top to bottom, rows represent (A) Day 2 0Gy, (B) Day 2 2Gy. Arrows examples of binding of IBA1 or TSPO antibodies. The blue in IBA1 and TSPO represents DAPI staining; the green represents the fluorophore Alexa Fluor 488, and indicates the binding of IBA1 and TSPO antibodies respectively.

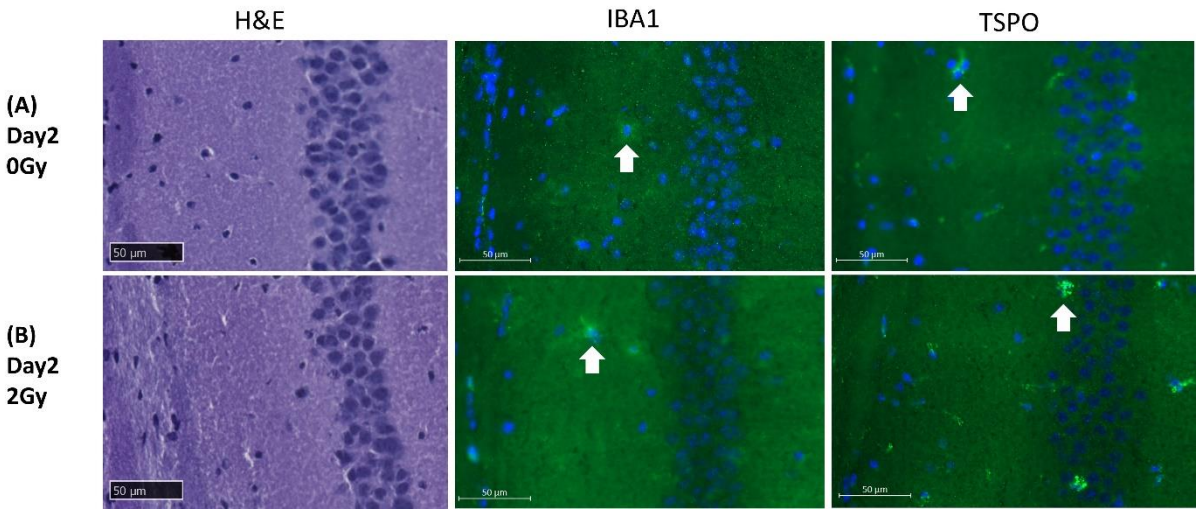

Figure 4. Left to right: H&E, IBA1 and TSPO immunofluorescence staining of radiotherapy hippocampus CA1 at 40x objective. Top to bottom, rows represent (A) Day 2 0Gy, (B) Day 2 2Gy. Arrows examples of binding of IBA1 or TSPO antibodies. The blue in IBA1 and TSPO represents DAPI staining; the green represents the fluorophore Alexa Fluor 488, and indicates the binding of IBA1 and TSPO antibodies respectively.

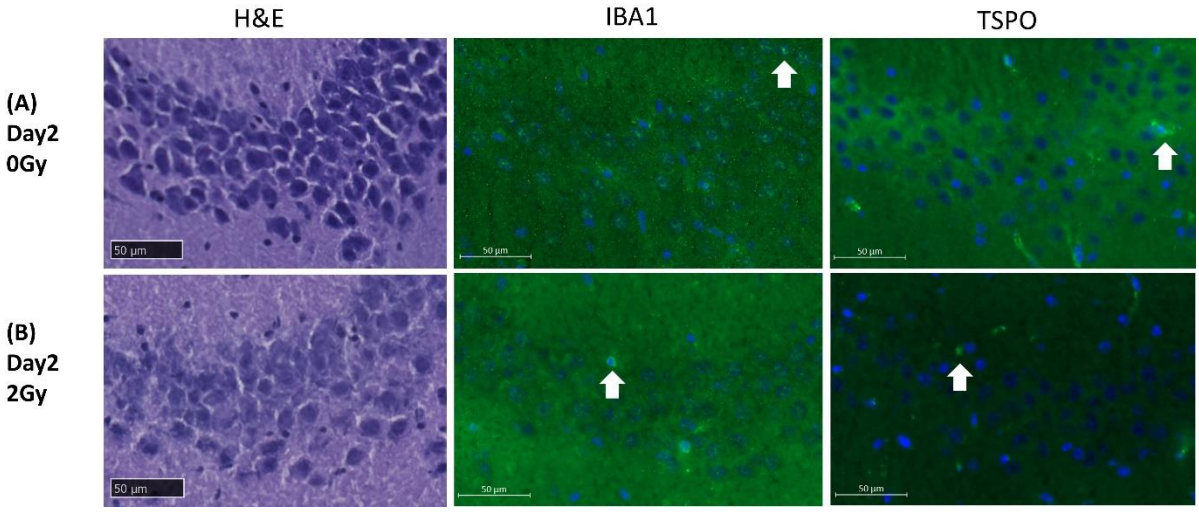

Figure 5. Left to right: H&E, IBA1 and TSPO immunofluorescence staining of the radiotherapy hippocampus CA3 at 40x objective. Top to bottom, rows represent (A) Day 2 0Gy, (B) Day 2 2Gy. Arrows examples of binding of IBA1 or TSPO antibodies. The blue in IBA1 and TSPO represents DAPI staining; the green represents the fluorophore Alexa Fluor 488, and indicates the binding of IBA1 and TSPO antibodies respectively.

6.1.1 Chemotherapy counts

From the chemotherapy counts data (Figure 6), there was predominantly no significant changes to IBA1 expression, except between Day 1 vs 32 controls of the prefrontal cortex (Figure 6; E). TSPO consistently showed significant increases in expression at later cull time points in both the treated and control animals (Figure 6; B, D, F).

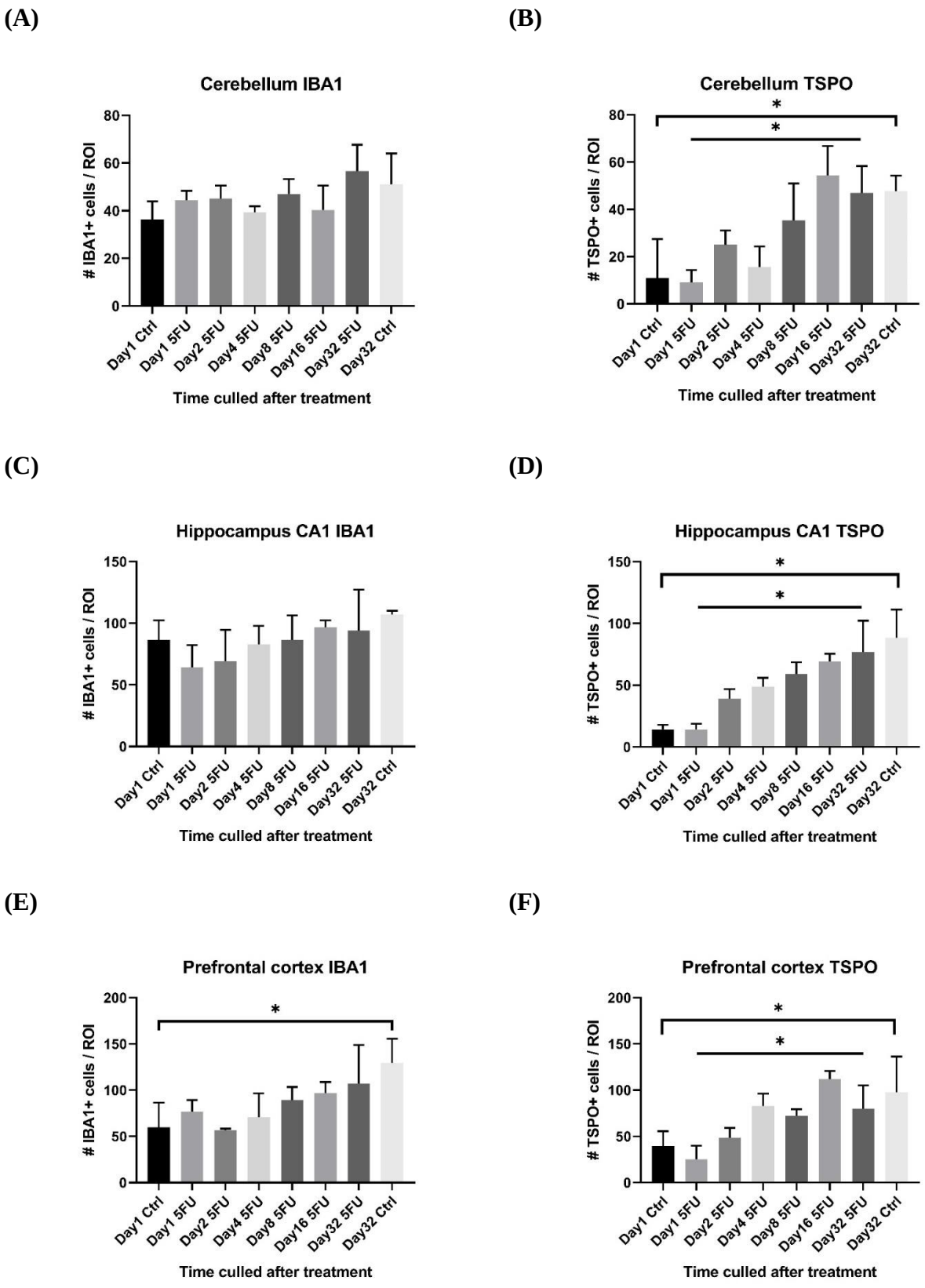

Figure 6. Number of IBA1+ (A, C, E) and TSPO+ (B, D, F) cells following 5FU chemotherapy per ROI 0.06mm^2. N=24. Statistical analyses via One-Way ANOVA and Tukey's multiple

comparisons. Significance P≤0.05 (*) and data represented as mean ± SD. No significance seen in IBA1 staining for cerebellum **(A)** and hippocampus CA1 **(C)**. Significance was seen for IBA1 prefrontal cortex **(E)** Day1 vs 32 Ctrl (P=0.034); TSPO cerebellum **(B)** Day1 vs 32 Ctrl (P=0.019), Day1 vs 16 and 32 5FU (P=0.0025 and 0.012), and Day4 vs 16 5FU (P=0.011); TSPO hippocampus CA1 **(D)** Day1 vs 32 Ctrl (P=0.0001), Day1 vs 8, 16 and 32 (P=0.016, 0.0025 and 0.0007); and TSPO prefrontal cortex **(F)** Day1 vs 32 (P=0.034), Day1 vs 4 and 16 (P=0.037 and 0.0010), and Day2 vs 16 (P=0.018).

6.1.2 Radiotherapy counts

There were no significant changes in the IBA1+ or TSPO+ counts from the radiotherapy tissue between 0 and 2 Gy radiation in the hippocampus regions dentate gyrus, CA1 and CA3 (Figure 7). The radiotherapy counts were compared alongside the most feasible corresponding chemotherapy counterparts. The chemotherapy IBA1+ cell counts were observed to be higher than the corresponding radiotherapy counts, which may be due to the different planes of sectioning, and indicates that chemo- and radiotherapy groups are not comparable. Significant increases were seen in the TSPO+ cell counts for CA1 and CA3.

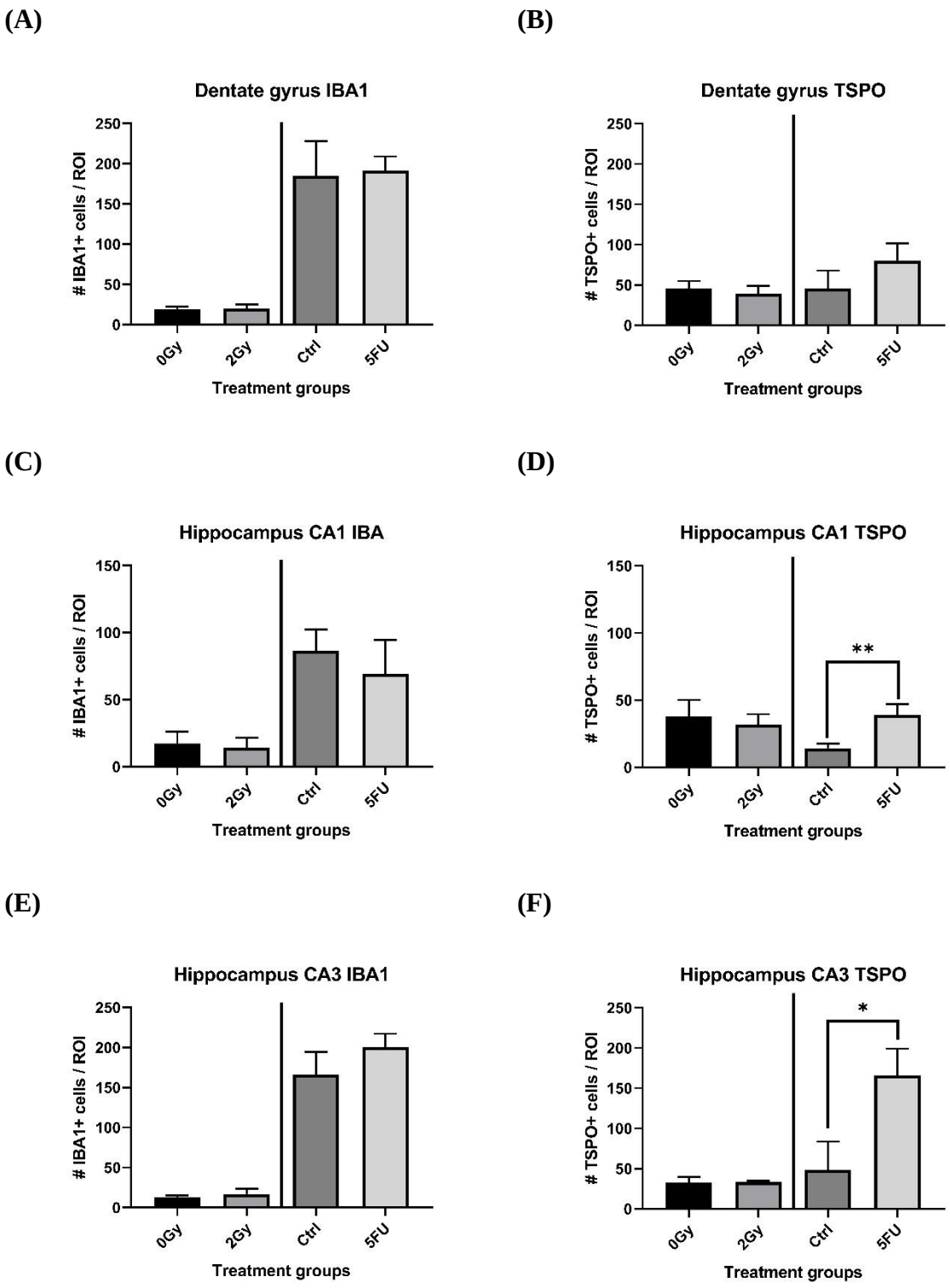

Figure 7. Number of IBA1+ (A, C, E) and TSPO+ (B, D, F) cells following either radio- or chemotherapy therapy (rad) per ROI 0.06mm^2. N=3-4/group. Statistical analyses via unpaired, parametric, two-tailed t-test. Significance *P≤0.05, **P≤0.01 and data represented as mean ± SD. Significance observed in hippocampus CA1 TSPO **(D)** Day1 Ctrl vs Day2 5FU (P= 0.0079); and

hippocampus CA3 TSPO **(F)** Day1 Ctrl vs Day2 5FU (P= 0.014). No significance observed in dentate gyrus IBA1 **(A)** and TSPO **(B)**; hippocampus CA1 IBA1 **(C)**; and hippocampus CA3 **(E)**.

6.2 IBA1+ microglia morphology

6.2.1 Chemotherapy morphology

Immunofluorescence staining for IBA1 had superior observable definition of ramified/resting microglia compared to TSPO (Figure 1). Morphology index ratios were quantified for chemotherapy IBA1 cerebellum, hippocampus dentate gyrus, CA1 and CA3, and prefrontal cortex. and represented as average ratio values (Figure 8).

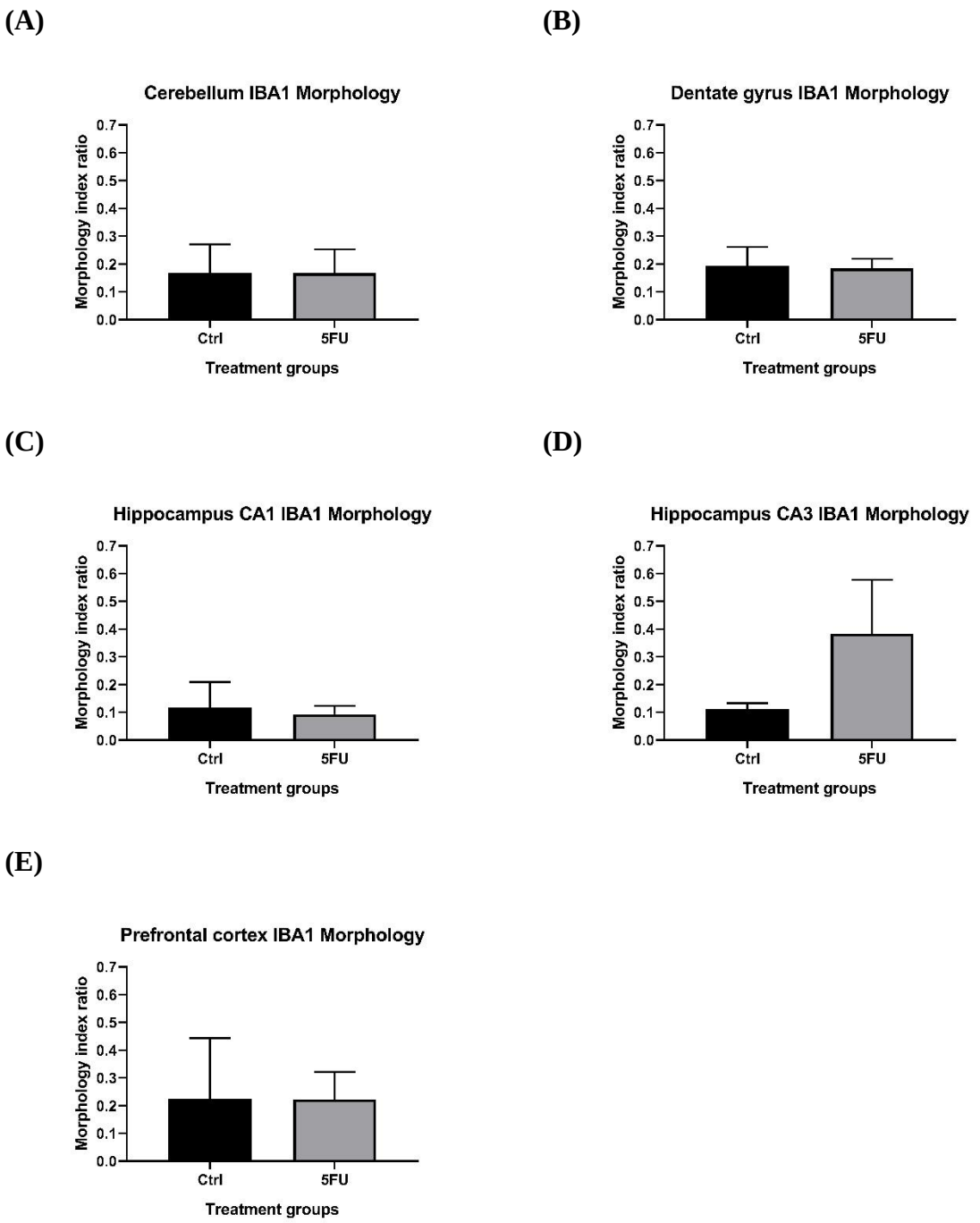

Figure 8. Morphology index ratio of IBA1+ cells following 5FU treatment. Statistical analyses via unpaired, parametric, two-tailed t-test. Significance *P≤0.05, and data represented as mean ± SD. No significance was observed in cerebellum **(A)** Day1 Ctrl vs Day2 5FU; dentate gyrus **(B)** Day1 Ctrl vs Day2 5FU; hippocampus CA1 **(C)** Day1 Ctrl vs Day2 5FU; hippocampus CA3 **(D)** Day1 Ctrl vs Day2 5FU; and prefrontal cortex **(E)** Day1 Ctrl vs Day2 5FU.

7. Discussion

This is the first study to investigate TSPO expression in multiple brain regions of mice treated with 5FU and total body irradiation, respectively.

7.1 No detectable microglia activation in IBA1+ and TSPO+ chemotherapy counts

For the chemotherapy study, lack of significant change in IBA1 expression, as well as the increase of TSPO expression from the Day 1 to 32 control, did go against current literature. Most studies have observed significant changes in IBA1 expression following chemotherapy. Interestingly, in human Alzheimer's models, IBA1+ cell counts predominantly did not change between the affected and control samples with increased microglia activation[13]. While the comparison is questionable due to the different models, it does highlight the lack of clarity surrounding detecting microglial activation. TSPO expression should not be largely detectable in microglia in otherwise healthy brains[20]. Combining the IBA1 and TSPO results indicates that either the absence or presence of microglia activation are plausible. A potential explanation for a lack of microglia activation is that TSPO staining highlighted cells beyond activated microglia, such as astrocytes, endothelial cells or pericytes, which have been seen to express TSPO when co-labelled with GFAP, CD31 and PDGFRβ respectively[23, 24]. Further, it has been suggested that increases in astrocyte TSPO expression precedes microglia TSPO expression in an Alzheimer's disease model[23]. On the other hand, a potential explanation for a presence of microglia activation is that while the overall number of microglia was unchanged with treatment, there was an increased proportion of activated microglia. This would be consistent with the results reported by Seigers et al. 2010[7] where the proportion of activated microglia increased after treatment with methotrexate compared to controls, as well as that of the human Alzheimer's models[13]. If there was indeed microglia activation, it is more likely to be explained by the stress from handling of the animals than the chemotherapy due to the observed increase in the TSPO expression of the controls. This would be parallel to the study conducted by Iwata et al. 2016 which reported that hippocampal microglia in rats activated in response to stress two days after attaining learned helplessness, and

further, while total number of microglia did not significantly change, the number of activated microglia significantly increase[29].

7.2 No significant changes in morphology in IBA1+ cells following chemotherapy

There were no significant changes in the morphology index ratio of IBA1+ cells in the chemotherapy groups between Day 1 control vs Day 2 5FU, cerebellum, hippocampus regions dentate gyrus, CA1 and CA3, and prefrontal cortex. Most studies that address microglia morphology are based on observation rather than quantification which complicates comparison between our results. Seigers et al. (2010) reported increased proportion of activated microglia, determined via observed morphology, significantly increased at 1 and 3 weeks after methotrexate treatment in the hippocampus compared to controls[7]. Similarly, Feiock et al. (2016)[3] reported higher number of activated microglia with larger cell bodies and thicker processes 3 days after methotrexate in areas including the hippocampus and cerebellum compared to controls. These studies suggest that our method of morphological analysis was insufficient to detect change in response to chemotherapy.

7.3 No significant changes between radiotherapy sham and treated

There were no significant changes between the radiotherapy sham (0 Gy control) and treated (2 Gy) animals. This is consistent with unpublished preliminary data from the laboratory of our collaborators. In comparison however, Feiock et al. (2016) treated mice with 16 Gy radiation to one hind limb and observed a significant increase to IBA1+ microglia in the hippocampus at Day 3[3]. This suggests that our model was insufficient to produce significant changes in microglia.

7.4 Radiotherapy cell counts were not comparable to chemotherapy counts

The IBA1+ chemotherapy counts for the hippocampus regions dentate gyrus, CA1, and CA3 were consistently higher than the corresponding radiotherapy counts. This indicates that the chemo- and radiotherapy counts were not comparable, which may be linked to a multitude of diverging variables, the most likely being the different sectioning planes, and perhaps the tissue preparation.

The results are contrary to Feiock et al 2016, which found no statistical significance between total number of microglia following methotrexate and NBRT after 3 days[3].

7.5 Comparison of our IBA1+ cell counts to literature

Seiger et al. 2016 investigated IBA1+ cell counts in response to 5FU. They reported, no significant differences in control vs 75mg/kg 5FU in the hippocampus after 3 and 15 weeks, and a significant decrease in from control to 5FU after 3 weeks in the prefrontal cortex, from 40 μm unspecified-plane sections in male mice[8]. After appropriate conversion to match the parameters of our study, our IBA1+ cell counts are proportionally higher in both the treated and controls for the hippocampus and prefrontal cortex. This indicates the potential of overcounting IBA1+ cells in our study.

7.6 Limitations strengths

The main limitation of our study was that IBA1 was not co-labelled with TSPO, CD68, or other antibodies associated with activated microglia. This made it impossible to identify which microglia were activated, and further to what extent did TSPO stain cells beyond microglia.

While this study was limited to only two control points at Day 1 and 32, it was enough to enable the identification of the potential handling and stress confounder. This could potentially be resolved by reducing animal handling with automatic weighing mechanisms in housing cages[30]. There were various inconsistencies between the chemo- and radiotherapy studies, which prevents meaningful comparisons between the two treatments. Most prominently, the tissue collection, processing and sectioning were contrary, paraffin-embedded sagittal for the chemotherapy study, and snap-frozen coronal for the radiotherapy. This is likely to have impacted the extent that IBA1 and TSPO were detected in the tissues; chemotherapy tissue had consistently higher IBA1+ counts compared to radiotherapy in the controls. Brain sections were at different planes, sagittal for the chemotherapy study and coronal radiotherapy. This barred comparison of the cerebellum and prefrontal cortex between the treatments, and only enabled comparison for the hippocampus regions. Further, the animals were of opposite genders, female for the chemotherapy study, and

male for radiotherapy, which may have had impacts on microglia. An old study conducted by Mouton et al. (2002) reported that female mice 25-40% higher numbers of microglia and astrocytes compared to age-matched male mice[31]. While this study may explain the higher number of IBA1+ cells in the corresponding chemotherapy animals to the radiotherapy counts, this requires confirmation with more recent studies and modern techniques.

Using tumour-free animals is both a limitation and strength. It brings to question the clinical relevance of our study as cancer treatment is given to patients with tumours, however it is a strength as tumour presence could not act as a confounder, as it alone has been seen to contribute to cognitive impairments[32, 33] and increased microglia activation[34, 35].

7.7 Future directions

In future, using multiple measures to identify activated microglia will ensure more confidence in results. Co-labelling of IBA1 and TSPO to reveal where they overlap would facilitate distinguishing microglia from astrocytes and endothelial cells, and would increase the accuracy of the TSPO counts data. Alternatives would be to co-label with GFAP, CD31, PDGFRβ to discount astrocytes, endothelial cells, and pericytes from the TSPO counts[24]. Further, assessing the IL12/10 ratio of samples may be valuable in confirming the presence of pro-inflammatory microglia, which secrete IL12, over anti-inflammatory microglia, which secrete IL10[5].

Ultimately, live imaging with a TSPO radiotracer to track changes to TSPO expression would be valuable in determining the feasibility of use in a clinical setting. Limited studies, have availed the use of radiotracers to identify microglial activation induced by cancer therapies. Parente et al. 2020[11] investigated the uptake of [^{11}C]PK11195, a TSPO radiotracer, in the brain after varying concentrations of whole-brain radiation in rats. The study identified comparable uptake on Day 3 between the treated and control groups, but found that on Day 31, the 25 Gy group had significantly higher uptake than the 10 Gy and control groups. However, [^{11}C]PK11195 is believed to lack sensitivity in detecting microglial activation at low levels[36], which may explain the lack of significant difference on Day 3. Alternative TSPO radiotracers exists, including [^{18}F]-DPA-713,

which has been shown to be specific to proinflammatory glial cells[19]; as well as flutriciclamide ([^{18}F]GE180), which has good affinity for TSPO[37] and has been used in multiple sclerosis[38] and Alzheimer's disease[39] animal models. However, both require further study to validate its feasibility to measure microglial activation induced by chemo- and radiotherapy.

Pannell et al. 2020 have used TSPO radiotracer [^{18}F]-DPA-713 *in vivo* along with *in vitro* methods to confirm upregulated TSPO expression in pro-inflammatory glia detection. Currently, no studies have investigated the use of the TSPO radiotracer [^{18}F]GE180 in *in vivo* and *in vitro* imaging to compare and contrast microglial activation induced by chemo- and radiotherapy respectively. Further investigation of TSPO radiotracers may enable researchers to determine the timing and location of neuroinflammation, which can be used to improve target interventions.
The outcome measures of our study were relatively subjective. To improve reliability of the cell count results, future studies could ensure there are at least two observers, which aligns with Seigers et al. 2010[7], where the values are not significantly different, and are averaged. Further, automating the morphology analysis may improve the reliability of the results[40]. Further optimisation of immunofluorescence staining, especially for IBA1 staining on frozen tissue, may reduce background in immunofluorescence images and maintain observable microglia processes.

7.8 Conclusion

Overall, for the chemotherapy tissue, IBA1+ cell counts did not significantly change in the cerebellum, hippocampus CA1 and prefrontal cortex. The TSPO+ cell counts increased with later cull time points in both the treated and the control animals for the cerebellum, hippocampus CA1 and prefrontal cortex, indicating that the results may be due to stress-related to handling. There were no significant changes between radiotherapy treated and controls in the hippocampus regions dentate gyrus, CA1 and CA3. Additionally, there were no significant changes in the morphology index ratio between Day 1 control and Day 2 5FU in the cerebellum, hippocampus regions dentate gyrus, CA1 and CA3, and prefrontal cortex.

Word count: 4487

8. Professional & Funding Acknowledgements

This research is supported by the AINSE Honours Scholarship Program.

Immunofluorescence and H&E staining images were obtained from Adelaide Microscopy facilities.

Special thanks to Courtney Subramaniam, Ghanyah Hamid Hussein Al-Qadami (PhD candidates) and Ines Semendric (laboratory technician), as well as all the members of the Cancer Toxicities Treatment Group, for assistance in animal work, tissue collection and preparation, as well as immunofluorescence staining; and to Agatha Labrinidis and Jane Sibbons for microscopy training and guidance.

9. References (~50)

1. Allen DH, Myers JS, Jansen CE, Merriman JD & Von Ah D (2018). Assessment and management of cancer- and cancer treatment–related cognitive impairment. *J Nurse Pract* **14**. 217-224.
2. Deprez S, Amant F, Yigit R, Porke K, Verhoeven J, Stock JVd, Smeets A, Christiaens M-R, Leemans A, Hecke WV, Vandenberghe J, Vandenbulcke M & Sunaert S (2011). Chemotherapy-induced structural changes in cerebral white matter and its correlation with impaired cognitive functioning in breast cancer patients. *Hum Brain Mapp* **32**. 480-493.
3. Feiock C, Yagi M, Maidman A, Rendahl A, Hui S & Seelig D (2016). Central nervous system injury – a newly observed bystander effect of radiation. *PLoS One* **11**.
4. Dey D, Parihar VK, Szabo GG, Klein PM, Tran J, Moayyad J, Ahmed F, Nguyen Q-A, Murry A, Merriott D, Nguyen B, Goldman J, Angulo MC, Piomelli D, Soltesz I, Baulch JE & Limoli CL (2020). Neurological impairments in mice subjected to irradiation and chemotherapy. *Radiat Res* **193**. 407-424.
5. Jurga AM, Paleczna M & Kuter KZ (2020). Overview of general and discriminating markers of differential microglia phenotypes. *Front Cell Neurosci* **14**.
6. Gibson EM, Nagaraja S, Ocampo A, Tam LT, Wood LS, Pallegar PN, Greene JJ, Geraghty AC, Goldstein AK, Ni L, Woo PJ, Barres BA, Liddelow S, Vogel H & Monje M (2019). Methotrexate chemotherapy induces persistent tri-glial dysregulation that underlies chemotherapy-related cognitive impairment. *Cell* **176**. 43-55.
7. Seigers R, Timmermans J, van der Horn HJ, de Vries EFJ, Dierckx RA, Visser L, Schagen SB, van Dam FSAM, Koolhaas JM & Buwalda B (2010). Methotrexate reduces hippocampal blood vessel density and activates microglia in rats but does not elevate central cytokine release. *Behav Brain Res* **207**. 265-272.
8. Seigers R, Loos M, Van Tellingen O, Boogerd W, Smit AB & Schagen SB (2016). Neurobiological changes by cytotoxic agents in mice. *Behav Brain Res* **299**. 19-26.

9. Blomstrand M, Kalm M, Grandér R, Björk-Eriksson T & Blomgren K (2014). Different reactions to irradiation in the juvenile and adult hippocampus. *Int J Radiat Biol* **90**. 807-815.

10. Constanzo J, Midavaine É, Fouquet J, Lepage M, Descoteaux M, Kirby K, Tremblay L, Masson-Côté L, Geha S, Longpré J-M, Paquette B & Sarret P (2020). Brain irradiation leads to persistent neuroinflammation and long-term neurocognitive dysfunction in a region-specific manner. *Prog Neuropsychopharmacol Biol Psychiatry* **102**.

11. Parente A, de Vries EFJ, van Waarde A, Ioannou M, van Luijk P, Langendijk JA, Dierckx RAJO & Doorduin J (2020). The acute and early effects of whole-brain irradiation on glial activation, brain metabolism, and behavior: A positron emission tomography study. *Mol Imaging Biol* **22**. 1012-1020.

12. Parihar VK, Acharya MM, Roa DE, Bosch O, Christie L-A & Limoli CL (2013). Defining functional changes in the brain caused by targeted stereotaxic radiosurgery. *Transl Cancer Res* **3**. 124-137.

13. Hopperton KE, Mohammad D, Trépanier MO, Giuliano V & Bazinet RP (2018). Markers of microglia in post-mortem brain samples from patients with Alzheimer's disease: a systematic review. *Mol Psychiatry* **23**. 177-198.

14. Jarmolowicz DP, Gehringer R, Lemley SM, Sofis MJ, Kaplan S & Johnson MA (2019). 5-Fluorouracil impairs attention and dopamine release in rats. *Behav Brain Res* **362**. 319-322.

15. Chaisawang P, Sirichoat A, Chaijaroonkhanarak W, Pannangrong W, Sripanidkulchai B, Wigmore P & Welbat JU (2017). Asiatic acid protects against cognitive deficits and reductions in cell proliferation and survival in the rat hippocampus caused by 5-fluorouracil chemotherapy. *PLoS One* **12**.

16. Choi SM, Lee SH, Yang YS, Kim BC, Kim MK & Cho KH (2001). 5-Fluorouracil-induced leukoencephalopathy in patients with breast cancer. *J Korean Med Sci* **16**. 328-334.

17. Matsumoto K, Nakajima T, Sakai H, Kato S, Sagara A, Arakawa K, Tashima K, Narita M & Horie S (2013). Increased expression of 5-HT3 and NK1 receptors in 5-fluorouracil-induced mucositis in mouse jejunum. *Dig Dis Sci* **58**. 3440-3451.

18. Betlazar C, Middleton RJ, Banati R & Liu G-J (2020). The translocator protein (TSPO) in mitochondrial bioenergetics and immune processes. *Cells* **9**.

19. Pannell M, Economopoulos V, Wilson TC, Kersemans V, Isenegger PG, Larkin JR, Smart S, Gilchrist S, Gouverneur V & Sibson NR (2020). Imaging of translocator protein upregulation is selective for pro-inflammatory polarized astrocytes and microglia. *Glia* **68**. 280-297.

20. Liu G-J, Middleton RJ, Hatty CR, Kam WW-Y, Chan R, Pham T, Harrison-Brown M, Dodson E, Veale K & Banati RB (2014). The 18 kDa translocator protein, microglia and neuroinflammation. *Brain Pathol* **24**. 631-653.

21. Milenkovic VM, Slim D, Bader S, Koch V, Heinl ES, Alvarez-Carbonell D, Nothdurfter C, Rupprecht R & Wetzel CH (2019). CRISPR-Cas9 mediated TSPO gene knockout alters respiration and cellular metabolism in human primary microglia cells. *Int J Mol Sci* **20**.

22. Denora N, Laquintana V, Trapani A, Suzuki H, Sawada M & Trapani G (2011). New fluorescent probes targeting the mitochondrial-located translocator protein 18 kDa (TSPO) as activated microglia imaging agents. *Pharm Res* **28**.

23. Tournier BB, Tsartsalis S, Ceyzériat K, Fraser BH, Grégoire M-C, Kövari E & Millet P (2020). Astrocytic TSPO upregulation appears before microglial TSPO in Alzheimer's disease. *J Alzheimers Dis* **77**. 1043-1056.

24. Betlazar C, Harrison-Brown M, Middleton RJ, Banati R & Liu GJ (2018). Cellular sources and regional variations in the expression of the neuroinflammatory marker translocator protein (TSPO) in the normal brain. *Int J Mol Sci* **19**.

25. Jelonek K, Krzywon A, Jablonska P, Slominska EM, Smolenski RT, Polanska J, Rutkowski T, Mrochem-Kwarciak J, Skladowski K & Widlak P (2020). Systemic effects of

radiotherapy and concurrent chemo-radiotherapy in head and neck cancer patients—comparison of serum metabolome profiles. *Metabolites* **10**. 60.

26. Wardill HR, Gibson RJ, Van Sebille YZA, Secombe KR, Coller JK, White IA, Manavis J, Hutchinson MR, Staikopoulos V, Logan RM & Bowen JM (2016). Irinotecan-induced gastrointestinal dysfunction and pain are mediated by common TLR4-dependent mechanisms. *Mol Cancer Ther* **15**. 1376-1386.

27. Wang H, Zhai K, Xue Y, Yang J, Yang Q, Fu Y, Hu Y, Liu F, Wang W, Cui L, Chen H, Zhang J & He W (2016). Global deletion of TSPO does not affect the viability and gene expression profile. *PLoS One* **11**.

28. Ibanez FG, Picard K, Bordeleau M, Sharma K, Bisht K & Tremblay M-È (2019). Immunofluorescence staining using IBA1 and TMEM119 for microglial density, morphology and peripheral myeloid cell infiltration analysis in mouse brain. *J Vis Exp* e60510.

29. Iwata M, Ishida H, Kaneko K & Shirayama Y (2016). Learned helplessness activates hippocampal microglia in rats: a potential target for the antidepressant imipramine. *Pharmacol Biochem Behav* **150-151**. 138-146.

30. Noorshams O, Boyd JD & Murphy TH (2017). Automating mouse weighing in group homecages with Raspberry Pi micro-computers. *J Neurosci Methods* **285**. 1-5.

31. Mouton PR, Long JM, Lei D-L, Howard V, Jucker M, Calhoun ME & Ingram DK (2002). Age and gender effects on microglia and astrocyte numbers in brains of mice. *Brain Research* **956**. 30-35.

32. Pyter LM, Cochrane SF, Ouwenga RL, Patel PN, Pineros V & Prendergast BJ (2010). Mammary tumors induce select cognitive impairments. *Brain Behav Immun* **24**. 903-907.

33. Yang M, Kim J, Kim J-S, Kim S-H, Kim J-C, Kang M-J, Jung U, Shin T, Wang H & Moon C (2014). Hippocampal dysfunctions in tumor-bearing mice. *Brain Behav Immun* **36**. 147-155.

34. Santos JC & Pyter LM (2018). Neuroimmunology of behavioral comorbidities associated with cancer and cancer treatments. *Front Immunol* **9**.

35. Norden DM, Bicer S, Clark Y, Jing R, Henry CJ, Wold LE, Reiser PJ, Godbout JP & McCarthy DO (2015). Tumor growth increases neuroinflammation, fatigue and depressive-like behavior prior to alterations in muscle function. *Brain Behav Immun* **43**. 76-85.

36. Sakata M, Ishibashi K, Imai M, Wagatsuma K, Ishii K, Hatano K, Ishiwata K & Toyohara J (2017). Assessment of safety, efficacy, and dosimetry of a novel 18-kDa translocator protein ligand, [11C]CB184, in healthy human volunteers. *EJNMMI Res* **7**.

37. Qiao L, Fisher E, McMurray L, Milicevic Sephton S, Hird M, Kuzhuppilly-Ramakrishnan N, Williamson DJ, Zhou X, Werry E, Kassiou M, Luthra S, Trigg W & Aigbirhio FI (2019). Radiosynthesis of (R,S)-[18F]GE387: A potential PET radiotracer for imaging translocator protein 18 kDa (TSPO) with low binding sensitivity to the human gene polymorphism rs6971. *ChemMedChem* **14**. 982-993.

38. Nack A, Brendel M, Nedelcu J, Daerr M, Nyamoya S, Beyer C, Focke C, Deussing M, Hoornaert C, Ponsaerts P, Schmitz C, Bartenstein P, Rominger A & Kipp M (2019). Expression of translocator protein and [18F]-GE180 ligand uptake in multiple sclerosis animal models. *Cells* **8**.

39. Liu B, Le KX, Park M-A, Wang S, Belanger AP, Dubey S, Frost JL, Holton P, Reiser V, Jones PA, Trigg W, Di Carli MF & Lemere CA (2015). In vivo detection of age- and disease-related increases in neuroinflammation by 18F-GE180 TSPO microPET imaging in wild-type and Alzheimer's transgenic mice. *J Neurosci* **35**. 15716-15730.

40. Young K & Morrison H (2018). Quantifying microglia morphology from photomicrographs of immunohistochemistry prepared tissue using ImageJ. *J Vis Exp* e57648.